Measuring Global, Direct, Diffuse, and Ground-Reflected Irradiance Using a Reference Cell Array

Michael Gostein[1], Adam Hoffman[2], Bruce H. King[3], Audrey Marquis[1]

[1]Atonometrics, Austin, USA; [2]Maxeon, San Jose, USA; [3]Sandia National Laboratories, Albuquerque, USA

Abstract **We report on an updated field trial of a novel method for measuring global horizontal irradiance (GHI), direct normal irradiance (DNI), diffuse horizontal irradiance (DHI), and reflected horizontal irradiance (RHI) using an array of reference cells with no moving parts. The technique, similar to previously explored methods using multi-pyranometer array concepts, uses multiple reference cells facing different directions together with an analysis model that fits the data from the sensors to determine GHI, DNI, DHI, and RHI. In previous work we reported on a first test of this approach at a single site. In this work we report further progress with this method, including an updated configuration of the reference cell array that offers improved sensitivity, an updated analysis that does not require site-specific training, and early field test results from prototypes installed at two different locations with different latitude.**

Index Terms **— photovoltaic systems, resource assessment, pyranometer, reference cell**

I. Introduction

Key steps in financing, commissioning, and monitoring commercial solar photovoltaic (PV) power plants require measurements of solar irradiance to predict and assess plant performance. Solar irradiance has multiple components, including direct, diffuse, and ground-reflected light. As PV systems become more sophisticated, especially for bifacial systems, there is an increasing need for more sophisticated irradiance measurements that resolve all irradiance components.

The most complete assessments of solar irradiance include determination of beam, diffuse, and ground-reflected components – e.g., direct normal irradiance (DNI), diffuse horizontal irradiance (DHI), and reflected horizontal irradiance (RHI) – which allows determination of irradiance on any plane via transposition. However, due to the cost and maintenance requirements of specialized equipment for DNI and DHI measurement, which usually involves moving parts for sun tracking, these measurements are typically omitted.

Pre-construction resource assessment campaigns typically only measure global horizontal irradiance (GHI), using a horizontally oriented thermopile pyranometer, and (with the increasing importance of bifacial PV systems) reflected horizontal irradiance (RHI), using a downfacing pyranometer or reference cell. Performance modeling software then employs decomposition models [1], such as DIRINT [2], to estimate DNI and DHI from GHI, followed by transposition models [1] to determine plane-of-array (POA) irradiance. However, the uncertainty of resource assessments and performance predictions may be increased due to reliance on decomposition models to determine diffuse irradiance.

Meteorological stations at built PV power plants typically include direct measurements of POA in addition to GHI [3], with GHI used for connection to plant design predictions and POA for monitoring of resource on the module plane. However, explicit measurement of direct and diffuse irradiance could reduce uncertainties in performance assessment, by allowing more accurate treatment of angle of incidence losses and, for bifacial systems, enabling better predictions of rear-side irradiance.

Here we discuss a novel method to provide a more complete irradiance assessment at lower cost. The method uses an array of multiple reference cells to determine GHI, DNI, DHI, and RHI, with no moving parts. The method is similar to that used in previous work on multi-pyranometer arrays [4][5][6]. However, in this work we use PV reference cells instead of pyranometers, we introduce a correction for incidence angle dependence of the sensors, and we explicitly measure and correct for ground-reflected irradiance instead of blocking it with a horizon blocking ring. In addition, we have implemented a fast calculation using a combination of simple models. Since our calculation determines the beam component of irradiance, it allows the effect of the sensor's incidence angle response



Fig. 1. Updated reference cell array prototype installed at Sandia National Laboratories, with five sky-facing reference cells (center, north, east, south, west) and one downfacing cell (on extension arm).

[7][8][9] to be automatically compensated, enabling accurate measurements of GHI with reference cells.

Previous work [10] reported on a first field test of a prototype reference cell array with measurements for direct and diffuse irradiance compared to research-grade systems. The study relied on a neural network model that was tuned for the specific site under study. We have since updated the reference cell array configuration to offer better sensitivity at all latitudes and have replaced the neural network model with an explicit calculation that is site independent.

Here we report early field test results of the new concept, with prototypes deployed at two different locations. Results are evaluated with several metrics, including comparison to research-grade measurements of direct and diffuse light and assessment of accuracy of PV system plane-of-array irradiance prediction.

II. Experiment

The new reference cell array concept includes 5 sky-facing reference cells, with four cells facing nominally north, east, south, and west on a 35-degree tilt and a central cell at a 5-degree south-facing tilt. Using a sensitivity analysis that considered the minimum difference in solar angle of incidence between any pair of reference cells, we determined that this configuration would have good sensitivity at all latitudes corresponding to typical installation locations. The central cell is intended to be nominally horizontal, with a 5-degree tilt for water roll off.

A prototype design is shown in Fig. 1. The prototype is assembled from existing PV reference cells (Atonometrics, RC18) and is intended to provide proof-of-concept. Following successful proof-of-concept a more compact productized version will be produced. The prototype also includes an additional downfacing reference cell mounted on an extension arm for measuring reflected horizontal irradiance (RHI) and albedo (RHI / GHI).

In March 2022, two similar prototypes were installed for field testing, one at the SunPower research and development facility near Davis, California, and one at Sandia National Laboratories in Albuquerque, New Mexico. Both sites also include a research-grade two-axis sun-tracking system (Kipp & Zonen, SOLYS) with a pyrheliometer and a shaded pyranometer for DNI and DHI measurement, as well as separate pyranometers for GHI measurement. The output of the reference cell arrays is evaluated against data from these reference instruments.

All the RC18 reference cells were calibrated at Atonometrics against an NREL-traceable reference cell on a class A solar simulator prior to the start of data collection.

In both installations the reference cell array is mounted at the edge of an elevated meteorological station platform approximately 4 meters off the ground. In the SunPower installation the platform edge is aligned east-west, the north reference cell faces the open side of the platform, and the downfacing reference cell is mounted directly underneath the five sky-facing reference cells. In the Sandia installation, the platform edge is aligned north-south, the west reference cell faces the open edge of the platform, and the down-facing reference cell is mounted on an arm extending off the platform over a paved area, as shown in Fig. 1.

The reference cell tilt angles were measured immediately following installation and confirmed to be within 1 degree of the design values. Reference cell azimuth angles were measured at installation using a compass; however, adjustments to azimuthal orientation values were made in post-processing the data by performing a best-fit of simulated to measured data on a single clear day at each site.

Data presented here were collected between mid-March and mid-April 2022 over about five weeks at each site.

Data are collected from all instruments on a one-minute or five-minute scan rate. Raw data from the reference cell array are recorded and then analyzed offline to determine results for DNI, DHI, GHI, and RHI. Offline calculations run on a personal computer and are implemented in MATLAB using the Sandia PVLIB toolbox [11].

III. Analysis Method

A. Nomenclature

Refer to Table 1 for a summary of nomenclature.

B. Basic model

Our goal is to determine DNI, DHI, and RHI at each time point by analyzing the readings of the six reference cells in the reference cell array.

At each time point we collect the irradiance readings of the six reference cells into a vector $\boldsymbol{B}$, where B_i is the reading of the ith reference cell. Now we relate the unknowns DNI, DHI, and RHI to the B_i values by

$$\begin{bmatrix} B_1 \\ B_2 \\ B_3 \\ B_4 \\ B_5 \\ B_6 \end{bmatrix} = \begin{bmatrix} A_{11} & A_{12} & A_{13} \\ A_{21} & A_{22} & A_{23} \\ A_{31} & A_{32} & A_{33} \\ A_{41} & A_{42} & A_{43} \\ A_{51} & A_{52} & A_{53} \\ A_{61} & A_{62} & A_{63} \end{bmatrix} \cdot \begin{bmatrix} \mathrm{DNI} \\ \mathrm{DHI} \\ \mathrm{RHI} \end{bmatrix} \quad (1)$$

where $\boldsymbol{A}$ is a matrix of sensitivity factors. Represented more simply,

$$\boldsymbol{B} = \boldsymbol{A} \cdot \boldsymbol{x} \quad (2)$$

where $\boldsymbol{x}$ is the vector (DNI, RHI, RHI).

The columns of $\boldsymbol{A}$ quantify, respectively, sensitivity of each reference cell to DNI, DHI, and RHI, and each row of $\boldsymbol{A}$ corresponds to reference cell i. Values of the sensitivity factors in $\boldsymbol{A}$ depend on the reference cell orientation and the solar position at each moment in time.

We calculate the left-most (DNI) column of $\boldsymbol{A}$ as

$$A_{i1} = IAM(\theta_i) \cdot \cos\theta_i \quad (3)$$

where θ_i is the solar angle of incidence on reference cell *i*, and $IAM(\theta_i)$ is the incidence angle modifier function of the reference cell for beam radiation. *IAM* expresses the deviation of an irradiance sensor from pure cosine dependence [7][8] and it should be determined experimentally, as discussed below.

For the middle (DHI) column of $\boldsymbol{A}$, we begin by assuming diffuse light is isotropically distributed in the sky dome, such that

$$A_{i2} = IAM_{diff} \cdot \left(\frac{1+\cos\beta_i}{2}\right) \quad (4)$$

where the term in parentheses quantifies the reduction in diffuse light received from the sky as the reference cell's tilt angle β_i increases, and IAM_{diff} quantifies the reduction in a reference cell's reading due to the distribution of incidence angles from the isotropically distributed diffuse light. IAM_{diff} is calculated by averaging $IAM(\theta_i)$ over the sky dome such as in [12].

We calculate the final (RHI) column of $\boldsymbol{A}$ by assuming ground-reflected light is diffuse and isotropically distributed (Lambertian reflectance), such that

$$A_{i3} = IAM_{diff} \cdot \left(\frac{1-\cos\beta_i}{2}\right) \quad (5)$$

where the term in parentheses quantifies the fraction of ground-reflected diffuse light that is captured by the reference cell as a function of its tilt angle.

At each time point we calculate the solar position and corresponding angle of incidences, calculate the matrix $\boldsymbol{A}$ per above, and calculate

$$\boldsymbol{x} = \boldsymbol{B}/\boldsymbol{A} \quad (6)$$

using a least-squares solution method [13], yielding results for DNI, DHI, and RHI.

C. Anisotropic Diffuse Model

To improve accuracy for DHI determination, we consider the anisotropic distribution of diffuse light in the sky dome, replacing eq. (4) with

$$A_{i2} = IAM_{diff} \cdot f_P(\mathrm{DNI}, \mathrm{DHI}, H, Z, \gamma, AM, \beta_i, \alpha_i) \quad (7)$$

where f_P is calculated using the empirical Perez sky diffuse model [14] in the PVLIB toolbox [15]. To calculate f_P, we use the Perez sky diffuse model to calculate the diffuse irradiance falling on the plane with tilt β_i and azimuth α_i (i.e. the reference cell plane) for given DNI, DHI, and other input parameters listed and then normalize by the DHI value. This provides the slope of A_{i3} with respect to small changes in DHI.

However, note that the calculation of f_P requires DNI and DHI, which are two of our three unknowns. Therefore, we perform the complete analysis in two stages. In the first stage, we construct $\boldsymbol{A}$ using the isotropic diffuse model in eq. (4) and then solve eq. (6), yielding an initial estimate for $\boldsymbol{x}$. In the second stage, we use the estimates for the DNI and DHI components of $\boldsymbol{x}$ to construct $\boldsymbol{A}$ again using eq. (7) and then repeat the solution per eq. (6).

Table 1. Summary of nomenclature

Global horizontal irradiance	GHI
Direct normal irradiance	DNI
Diffuse horizontal irradiance	DHI
Reflected horizontal irradiance	RHI
Albedo	a
Solar zenith	Z
Solar azimuth	γ
Reference cell *i* tilt angle	β_i
Reference cell *i* azimuth angle	α_i
Solar angle of incidence to reference cell *i*	θ_i
Incidence angle modifier, beam radiation	$IAM(\theta_i)$
Incidence angle modifier, diffuse radiation	IAM_{diff}
Vector of irradiance readings	$\boldsymbol{B}$
Matrix of sensitivities	$\boldsymbol{A}$
Vector of unknowns (DNI, DHI, RHI)	$\boldsymbol{x}$
Extraterrestrial normal irradiance	H
Air mass	AM
Sensitivity to DHI in anisotropic model	f_P

D. GHI

Once DNI and DHI are determined, we calculate GHI per

$$\mathrm{GHI} = (\cos Z) \cdot \mathrm{DNI} + \mathrm{DHI} \quad (8)$$

E. Using Assumed Albedo

In place of directly solving for RHI, we can also modify the equations to use an assumed albedo *a*, which is the ratio RHI/GHI.

To do this, we construct $\boldsymbol{x}$ as the two-element vector (DNI, DHI) and eliminate the third column of $\boldsymbol{A}$ (see eq. (1)). Then we add

$$IAM_{diff} \cdot a \cdot (\cos Z) \cdot \left(\frac{1-\cos\beta_i}{2}\right) \quad (9)$$

to eq. (3) and add

$$IAM_{diff} \cdot a \cdot \left(\frac{1-\cos\beta_i}{2}\right) \quad (10)$$

to eq. (4) and eq. (7).

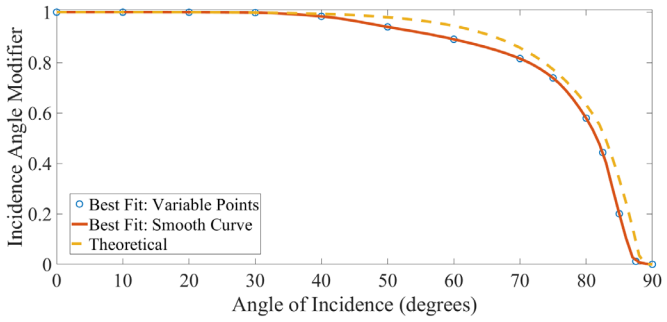


Fig. 2. Best fit vs. theoretical curves for reference cell incidence angle modifier $IAM(\theta_i)$.

IV. IAM Function

Accurate results require precise determination of the reference cell *IAM* functions. The primary factor determining $IAM(\theta_i)$ is reflection losses from the reference cell surface which can be calculated theoretically using the known indices of refraction of the reference cell glass, encapsulation, and silicon. However, geometric and other factors also modify the function. Our previous work [10], [16], [17] used a theoretically calculated curve for $IAM(\theta_i)$ which attempted to take into account both the optical and geometric properties of the RC18 reference cells. However, in this work, we empirically determined a new curve for $IAM(\theta_i)$ which produces a best fit to the tracking diffusometer data for DHI on a single clear day for the reference cell array installed at the SunPower location. Results are presented in Fig. 2. Differences between the theoretical and best-fit $IAM(\theta_i)$ curve likely explain some anomalies observed in previous work.

V. Results

A. Time Series

Fig. 3 displays an example set of results for GHI, DNI, DHI, and RHI determined from the reference cell array at the SunPower location over a four-day period. These data illustrate sensitivity to a range of diffuse irradiance levels on clear and cloudy days. The figure shows general agreement between the reference cell array results and those of the reference instruments. (Note there was no reference instrumentation for RHI.)

Results from the Sandia test site were similar, albeit with an anomaly that causes an asymmetry in the DHI profile on very clear days, resulting in DHI readings about 10-30 W/m^2 higher than expected during late afternoon hours. We suspect that the asymmetry is caused by the specific configuration of the reference cell array at the Sandia site as described in section II. The downfacing reference cell is located on an extension arm overhanging the meteorology platform to the west; therefore it sees shade in the morning and reflected light from the platform

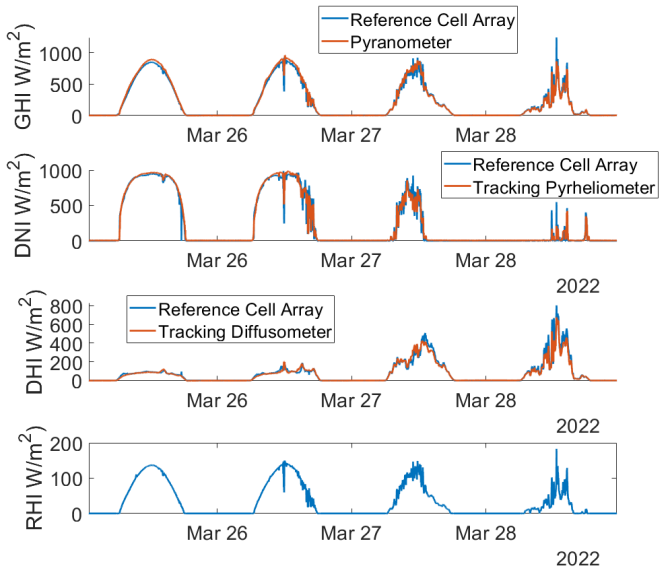


Fig. 3. Example reference cell array results from the SunPower site over a four-day period and comparison to reference instruments.

building wall in the afternoon. Furthermore, the west-facing cell of the array looks out over an open area west of the platform which may have higher albedo than the area to the east on top of the platform itself. These effects are under further investigation. However, as shown in the tables below, results from the Sandia station still generally agree well with the reference instrumentation, especially at higher DHI values corresponding to cloudy days.

B. Correlation to Reference Instruments

Table 3 summarizes the comparison of the reference cell array results to those from the reference instruments over the approximately five-week period at each site. The table shows mean-bias deviation (MBD) and root-mean-square deviation (RMSD) for hourly-averaged data, where the reference cell array results for GHI, DNI, and DHI are correlated against, respectively, data from the thermopile pyranometer, tracking pyrheliometer, and tracking diffusometer. For comparison, we also include statistics for correlation of DNI and DHI derived from the pyranometer GHI measurements via DIRINT decomposition [1] versus the DNI and DHI from the reference instruments.

The table generally shows good performance for the reference cell array, with low MBD in the range 0-2% for GHI, DNI, and DHI. One exception is the elevated MBD of 4.6% (5.6 W/m^2) for the DHI results at the Sandia site. This is likely due to the elevated reference cell array DHI results at this site on clear days during afternoon hours, as discussed above, which is under investigation. The reference cell array results generally correlate better to the reference instruments than those from the DIRINT decomposition. We expect that the relative benefit of the reference cell array versus decomposition alone would

Table 2: Correlation of hourly-averaged reference cell array and decomposition results with reference instrumentation over five-week trial.

Parameter	Reference Instrument	Reference Cell Array		DIRINT Decomposition	
		MBD W/m² (%)	RMSD W/m² (%)	MBD W/m² (%)	RMSD W/m² (%)
SunPower					
GHI	Thermopile Pyranometer	-2.3 (-0.5)	17.7 (3.8)	n/a	n/a
DNI	Tracking Pyrheliometer	1.2 (0.2)	47.6 (7.7)	43.5 (7.2)	64.6 (10.7)
DHI	Tracking Diffusometer	-0.9 (-0.6)	29.6 (21.8)	-24.0 (-17.7)	33.3 (24.5)
Sandia					
GHI	Thermopile Pyranometer	-8.6 (-1.7)	33.6 (6.5)	n/a	n/a
DNI	Tracking Pyrheliometer	-12.6 (-1.9)	42.1 (6.3)	12.4 (1.9)	65.0 (9.8)
DHI	Tracking Diffusometer	5.6 (4.6)	36.3 (29.5)	1.0 (0.8)	36.3 (29.4)

increase when evaluating data over longer time periods with more seasonal variation. Note, for example, that the decomposition-derived DHI in Table 3 shows a relatively poor MBD at the SunPower site (-17.7%) but an excellent value at the Sandia site (0.8%), while the reference cell array results for DHI are much more consistent at both sites, with MBD of -0.6% and 4.6%, respectively.

C. *POA Irradiance Prediction*

Since the goal of measuring DNI and DHI is to predict PV performance by calculating irradiance in a specific plane of array (POA), at each site we have evaluated the results by using the DNI and DHI to predict the POA irradiance measured by a reference cell on a tilted plane elsewhere on the site. The three DNI and DHI sources are the reference cell array, the reference instruments (tracking pyrheliometer and diffusometer), and DIRINT decomposition. The POA reference cell was south-facing at 25-degree tilt at the Sandia site and south-facing with 20-degree tilt at SunPower.

Table 3: Correlation of hourly-averaged predicted POA irradiance, using three different DNI and DHI sources, with measured POA reference cell irradiance measurement.

DNI & DHI Source for POA Prediction	Correlation to POA Reference Cell	
	MBD W/m² (%)	RMSD W/m² (%)
SunPower		
Reference Cell Array	-2.2 (-0.4)	15.4 (2.7)
Tracking Instruments	5.5 (1.0)	11.5 (2.1)
DIRINT Decomposition	5.1 (0.9)	14.0 (2.5)
Sandia		
Reference Cell Array	0.2 (0.0)	17.2 (3.3)
Tracking Instruments	6.7 (1.3)	25.5 (4.8)
DIRINT Decomposition	8.0 (1.5)	25.5 (4.8)

Table 2 presents the results of these tests. Predictions made using all three DNI and DHI sources have similar quality of correlation against the measured POA data. A close inspection of the data showed that small differences in RMSD were dominated by discrepancies between the instruments on cloudy days with high irradiance fluctuations, when differences in sensor position and acquisition timing result in non-correlation. To draw significant conclusions about the relative benefit of the reference cell array results versus decomposition analysis alone will require collection of data over a longer time.

In this work we assessed only the prediction of front-side POA. As we continue this investigation, we intend to assess the utility of the reference cell array data for predicting also rear-side POA irradiance that would be relevant to bifacial modules. Here consistency of DHI determination will be much more important.

VI. Ongoing Work

Data presented here were acquired over a limited period of approximately 5 weeks at each site. Data collection and analysis are continuing.

For this work, we determined a best-fit IAM function for the reference cells by optimizing the agreement between the reference cell and tracking diffusometer DHI results on one clear day at one site. However, we plan to directly measure the reference cell IAM outdoors as in [9] or with similar protocols. This will provide an independent basis for evaluating the reference cell array analysis and comparing results between sites. In addition, it could elucidate any anisotropic aspects of the reference cell angle of incidence response, which could then permit more accurate analysis.

Soiling could have a significant impact on the results by altering the IAM at high incidence angles. The potential uncertainty from this effect could be studied using a modeling approach, by considering angle-dependent shading due to dust particles at different soiling levels as in [18].

As discussed above, reference cell array results for DHI at Sandia showed anomalously high readings for late afternoon hours on very clear days. We are investigating potential reconfiguration of the array to eliminate this effect.

VI. Conclusions

We have demonstrated the potential to use a reference cell array, with no moving parts, to determine global, direct, diffuse, and ground-reflected radiation components. Updating on previous work with this concept [10], the analysis is now based on explicit calculation rather than training to reference data. The only site-specific data used for calibrating the technique were the data used to establish reference cell incidence angle response, and in upcoming work we plan to measure this response independently. Results at the two sites studied show good correlation between the reference cell array and high-quality reference instrumentation for GHI, DNI, and DHI.

Further work is ongoing. A successful outcome of this project would enable using a reference cell array to add capability to resource assessment campaigns and solar power plant meteorological stations at low cost.

ACKNOWLEDGEMENT

This material is based upon work supported by the U.S. Department of Energy's Solar Energy Technologies Office under Award Number DE-SC0020831.

Sandia National Laboratories is a multimission laboratory managed and operated by National Technology and Engineering Solutions of Sandia, LLC, a wholly owned subsidiary of Honeywell International Inc., for the U.S. Department of Energy's National Nuclear Security Administration under contract DE-NA0003525.

REFERENCES

[1] M. Lave, W. Hayes, A. Pohl, and C. W. Hansen, "Evaluation of global horizontal irradiance to plane-of-array irradiance models at locations across the United States," *IEEE J. Photovoltaics*, vol. 5, no. 2, pp. 597–606, Mar. 2015, doi: 10.1109/JPHOTOV.2015.2392938.

[2] P. Ineichen, R. Perez, R. Seal, E. Maxwell, and A. Zalenka, "Dynamic global-to-direct irradiance conversion models," *ASHRAE Trans.*, vol. 98, no. 1, pp. 354–369, 1992.

[3] "IEC 61724-1 Ed. 1.0 en:2017 - Photovoltaic system performance - Part 1: Monitoring."

[4] D. Faiman, D. Feuermann, and A. Zemel, "Site-independent algorithm for obtaining the direct beam insolation from a multipyranometer instrument," *Sol. Energy*, vol. 50, no. 1, pp. 53–57, Jan. 1993, doi: 10.1016/0038-092X(93)90007-B.

[5] B. Marion, "Multi-Pyranometer Array Design and Performance Summary," *Proc. 1998 Am. Sol. Energy Annu. Conf.*, 1998.

[6] J. C. Baltazar, Y. Sun, and J. Haberl, "Improved methodology to evaluate clear-sky direct normal irradiance with a multi-pyranometer array," *Sol. Energy*, vol. 121, pp. 123–130, Nov. 2015, doi: 10.1016/j.solener.2015.07.015.

[7] N. Martin and J. M. Ruiz, "Calculation of the PV modules angular losses under field conditions by means of an analytical model," *Sol. Energy Mater. Sol. Cells*, vol. 70, no. 1, pp. 25–38, Dec. 2001, doi: 10.1016/S0927-0248(00)00408-6.

[8] B. H. King and C. D. Robinson, "Differential Analysis of the Angle of Incidence Response of Utility-Grade PV Modules," in *2019 IEEE 46th Photovoltaic Specialists Conference (PVSC)*, Jun. 2019, pp. 77–81, doi: 10.1109/PVSC40753.2019.8981355.

[9] B. H. King, D. Riley, C. D. Robinson, and L. Pratt, "Recent advancements in outdoor measurement techniques for angle of incidence effects," *2015 IEEE 42nd Photovolt. Spec. Conf. PVSC 2015*, Dec. 2015, doi: 10.1109/PVSC.2015.7355849.

[10] M. Gostein, A. Hoffman, F. Farina, and B. Stueve, "Measuring Global, Direct, and Diffuse Irradiance Using a Reference Cell Array," in *Conference Record of the IEEE Photovoltaic Specialists Conference*, Jun. 2021, pp. 923–927, doi: 10.1109/PVSC43889.2021.9518735.

[11] "PV Performance Modeling Collaborative | PV_LIB Toolbox." https://pvpmc.sandia.gov/applications/pv_lib-toolbox/ (accessed Mar. 15, 2021).

[12] B. Marion, "Numerical method for angle-of-incidence correction factors for diffuse radiation incident photovoltaic modules," *Sol. Energy*, vol. 147, pp. 344–348, May 2017, doi: 10.1016/j.solener.2017.03.027.

[13] "Solve systems of linear equations Ax = B for x - MATLAB mldivide \." https://www.mathworks.com/help/matlab/ref/mldivide.html?s_tid=srchtitle (accessed May 19, 2022).

[14] R. Perez, P. Ineichen, R. Seals, J. Michalsky, and R. Stewart, "Modeling daylight availability and irradiance components from direct and global irradiance," *Sol. Energy*, vol. 44, no. 5, pp. 271–289, Jan. 1990, doi: 10.1016/0038-092X(90)90055-H.

[15] "PV Performance Modeling Collaborative | Perez Sky Diffuse Model." https://pvpmc.sandia.gov/modeling-steps/1-weather-design-inputs/plane-of-array-poa-irradiance/calculating-poa-irradiance/poa-sky-diffuse/perez-sky-diffuse-model/ (accessed May 19, 2022).

[16] M. Gostein, B. Stueve, R. Clark, P. Keelin, M. Grammatico, and M. Reusser, "Field Trial of Meteorological Station Using PV Reference Cells," in *Conference Record of the IEEE Photovoltaic Specialists Conference*, Jun. 2020, vol. 2020-June, pp. 0520–0523, doi: 10.1109/PVSC45281.2020.9300799.

[17] M. Gostein, R. Clark, M. Grammatico, P. Keelin, M. Reusser, and B. Stueve, "Updated Trial of Meteorological Station Using PV Reference Cell Array," *Conf. Rec. IEEE Photovolt. Spec. Conf.*, pp. 2357–2359, Jun. 2021, doi: 10.1109/PVSC43889.2021.9518743.

[18] J. Zorrilla-Casanova *et al.*, "Losses produced by soiling in the incoming radiation to photovoltaic modules," 2012, doi: 10.1002/pip.1258.